Theor Chem Account (2008) 120:107–118
DOI 10.1007/s00214-007-0311-9

REGULAR ARTICLE

Kinetics of the hydrogen abstraction CHO + Alkane → HCHO + Alkyl reaction class: an application of the reaction class transition state theory

Lam K. Huynh · **Thanh N. Truong**

Received: 20 November 2006 / Accepted: 12 February 2007 / Published online: 24 July 2007

Abstract The kinetics of the hydrogen abstraction at alkanes by formyl radicals is investigated using the reaction class transition state theory (RC-TST) approach combined with the linear energy relationship (LER) or the barrier height grouping (BHG). The rate constants of a reaction in this class can be estimated through those of the reference reaction, $CHO + C_2H_6$, which are obtained from rate constants of the reaction that involves the smallest species, namely $CHO + CH_4$, using the explicit RC-TST scaling. The thermal rate constants of this smallest reaction are evaluated at the canonical variational transition state theory (CVT) with the corrections from the small-curvature tunneling (SCT) and hindered rotation (HR) treatments. Our analyses indicate that less than 40% systematic errors, on the average, exist in the predicted rate constants using both the LER approach, where only reaction energy is needed, and the BHG approach, where no additional information is needed; while comparing to explicit rate calculations the differences are less than 60%.

Keywords Rate constant · Hydrogen abstraction by formyl radicals · Reaction class · Transition state theory · Hydrocarbon combustion

1 Introduction

Reactions belonging to the reaction class of formyl radicals with alkanes, CHO + RH → HCHO + R, are included in detailed kinetic models for simulating chemical processes, particularly for combustion of hydrocarbon fuels [1–4]. The availability for the rate constants of such reactions is limited, e.g., only indirect data exists for hydrocarbons up to C_4 (4 carbon-atom chains) [5–7]. For construction of global detailed kinetic mechanisms which consist of a great number of all possible reactions, rate constants of other reactions in this class are needed. Such global detailed kinetic mechanisms would be able to capture physical observations of different types of chemical reactors in various conditions.

The practicality of using the reaction class transition state theory (RC-TST) for estimating rate constants of a large number of reactions in a given reaction class has been applied successfully in several previous studies [8–11]. In this study we applied the RC-TST approach to derive all parameters for estimating the rate constants of any reaction belonging to this reaction class. To do so, our main task is to find analytical correlation expressions for the rate constants between reactions in a small representative set of the class and the reference one. These correlation expressions are applicable to all reactions in the class, and thus the rate constants of an arbitrary reaction in the class can be estimated relatively to those of the reference reaction.

To develop RC-TST parameters for the CHO + Alkane class, 15 reactions are considered as a representative set of reactions. These reactions are given below:

$$\begin{aligned}
CHO + CH_4 &\rightarrow HCHO + \underline{C}H_3 && (R_1)\\
CHO + CH_3CH_3 &\rightarrow HCHO + \underline{C}H_2CH_3 && (R_2)\\
CHO + CH_3CH_2CH_3 &\rightarrow HCHO + \underline{C}H_2CH_2CH_3 && (R_3)\\
&\rightarrow HCHO + CH_3\underline{C}HCH_3 && (R_4)\\
CHO + CH_3CH_2CH_2CH_3 &\rightarrow HCHO + \underline{C}H_2CH_2CH_2CH_3 && (R_5)\\
&\rightarrow HCHO + CH_3\underline{C}HCH_2CH_3 && (R_6)\\
CHO + (CH_3)_2CHCH_3 &\rightarrow HCHO + (CH_3)_2CH\underline{C}H_2 && (R_7)\\
&\rightarrow HCHO + (CH_3)_3\underline{C} && (R_8)
\end{aligned}$$

Contribution to Mark S. Gordon 65th Birthday Festschrift Issue.

L. K. Huynh · T. N. Truong (✉)
Department of Chemistry, University of Utah,
315 S. 1400 E. Rm. 2020, Salt Lake City, UT 84112, USA
e-mail: Truong@chem.chemistry.utah.edu

$$\begin{aligned}
\mathrm{CHO + CH_3CH_2CH_2CH_2CH_3} &\rightarrow \mathrm{HCHO} + \underline{\mathbf{C}}\mathrm{H_2CH_2CH_2CH_2CH_3} && (\mathrm{R}_9)\\
&\rightarrow \mathrm{HCHO + CH_3}\underline{\mathbf{C}}\mathrm{HCH_2CH_2CH_3} && (\mathrm{R}_{10})\\
&\rightarrow \mathrm{HCHO + CH_3CH_2}\underline{\mathbf{C}}\mathrm{HCH_2CH_3} && (\mathrm{R}_{11})\\
\mathrm{CHO + (CH_3)_2CHCH_2CH_3} &\rightarrow \mathrm{HCHO} + \underline{\mathbf{C}}\mathrm{H_2(CH_3)CHCH_2CH_3} && (\mathrm{R}_{12})\\
&\rightarrow \mathrm{HCHO + (CH_3)_2}\underline{\mathbf{C}}\mathrm{CH_2CH_3} && (\mathrm{R}_{13})\\
&\rightarrow \mathrm{HCHO + (CH_3)_2CH}\underline{\mathbf{C}}\mathrm{HCH_3} && (\mathrm{R}_{14})\\
&\rightarrow \mathrm{HCHO + (CH_3)_2CHCH_2}\underline{\mathbf{C}}\mathrm{H_2}, && (\mathrm{R}_{15})
\end{aligned}$$

where reactions (R_1), (R_2), (R_3), (R_5), (R_7), (R_9) (R_{12}) and (R_{15}) are hydrogen abstraction reactions at the primary carbons; (R_4), (R_6), (R_{10}), (R_{11}), and (R_{14}) are at the secondary carbons, and (R_8) and (R_{13}) are at the tertiary carbons; here bold underlined C letters represent radical sites as in the products of hydrogen abstraction reactions.

2 Methodology

2.1 Reaction class transition state theory (RC-TST)

Since the details of the RC-TST/LER method have been presented elsewhere [8,9,12–14], we discuss only its main features here. It is based on the realization that reactions in the same class have the same reactive moiety; thus the difference between the rate constants of any two reactions is mainly due to the difference in the interactions between the reactive moiety and their different substituents. Within the RC-TST framework, the rate constant of an arbitrary reaction (denoted as k_a) is proportional to that of the reference reaction, k_r, in the same class by a temperature dependent function f(T):

$$k_a(T) = f(T) \times k_r(T) \tag{1}$$

The rate constants for the reference reaction $k_r(T)$ are often known experimentally or can be calculated accurately from first-principles while $f(T)$ can be factored into different components under the TST framework as follows:

$$f(T) = f_\sigma \times f_\kappa \times f_Q \times f_V \tag{2}$$

where f_σ, f_κ, f_Q and f_V are symmetry number, tunneling, partition function and potential energy factors, respectively. These factors are simply the ratios of the corresponding components in the TST expression for the two reactions:

$$f_\sigma = \frac{\sigma_a}{\sigma_r} \tag{3}$$

$$f_\kappa(T) = \frac{\kappa_a(T)}{\kappa_r(T)} \tag{4}$$

$$f_Q(T) = \frac{\left(\frac{Q_a^{\neq}(T)}{\Phi_a^R(T)}\right)}{\left(\frac{Q_r^{\neq}(T)}{\Phi_r^R(T)}\right)} = \frac{\left(\frac{Q_a^{\neq}(T)}{Q_r^{\neq}(T)}\right)}{\left(\frac{\Phi_a^R(T)}{\Phi_r^R(T)}\right)} \tag{5}$$

$$f_V(T) = \exp\left[-\frac{(\Delta V_a^{\neq} - \Delta V_r^{\neq})}{k_B T}\right] = \exp\left[-\frac{\Delta\Delta V^{\neq}}{k_B T}\right] \tag{6}$$

where $\kappa(T)$ is the transmission coefficient accounting for the quantum mechanical tunneling effects; σ is the reaction symmetry number; $Q^{\neq}$ and Φ^R are the total partition functions (per unit volume) of the transition state and reactants, respectively; $\Delta V^{\neq}$ is the classical reaction barrier height; T is the temperature in Kelvin; k_B and h are the Boltzmann and Planck constants, respectively. The potential energy factor can be calculated using the reaction barrier heights of the arbitrary reaction and the reference reaction. The classical reaction barrier height $\Delta V^{\neq}$ for an arbitrary reaction can be obtained without having to calculate it explicitly by using the linear energy relationship (LER), which is similar to the Evans–Polanyi relationship [15–17] between classical barrier heights and reaction energies. As discussed below, such a barrier height can also be estimated by a grouping procedure denoted as barrier height grouping (BHG) that provides an average barrier height for a given sub-class of reactions.

The main tasks of this paper are: (1) to determine the explicit expressions for these factors linking the rate constants of R_r and those of R_a in the same class using a small representative set of reactions in the class as mentioned earlier; and (2) to provide error analyses of the results. Once these expressions are determined, the thermal rate constants of any reaction in this class can be predicted using (1) no additional information in the case of using the BHG approach, or (2) only the reaction energy in the case of using the LER expression.

It is worth mentioning that within the RC-TST framework, the re-crossing effect is only implicitly included in the rate constants of the reference reaction and is not explicitly included in the calculation of the reaction class factors.

2.2 Computational methods

All the electronic structure calculations were carried out using the program package GAUSSIAN03 [18]. A hybrid non-local density functional theory (DFT), particularly Becke's half-and-half (BH&H) [19] non-local exchange and Lee–Yang–Parr (LYP) [20] non-local correlation functionals, has been found previously to be sufficiently accurate for predicting the transition state properties for hydrogen abstraction reactions by a radical [21–23].

Note that within the RC-TST framework only the relative barrier heights are needed. Our previous study has shown that they can be accurately predicted by the BH&HLYP method [9,14]. Geometries of reactants, transition states, and products were optimized at the BH&HLYP level of theory with the Dunning's correlation-consistent polarized valence double-zeta basis set $[3s2p1d/2s1p]$ denoted as cc-pVDZ [24], which is believed to be large enough to capture the physical changes along the reaction coordinate for this type of reaction. Frequencies of the stationary points were also calculated at the same level of theory. This information was used to derive the RC-TST factors. The AM1 semi-empirical method was also employed to calculate the reaction energies of those reactions considered here. The AM1 and BH&HLYP/cc-pVDZ reaction energies were then used to derive the LERs between the barrier heights and reaction energies. It is worth mentioning that the AM1 reaction energies are only used to extract "accurate" barrier heights from the LERs; thus it is not directly involved in any rate calculations. Note that calculations of all open- and closed-shell species are carried out at un-restricted and restricted methods, respectively.

For the principal CHO + CH_4 reaction the minimum energy path (MEP) of the potential energy surface was also obtained at the BH&HLYP/cc-pVDZ level by following the Gonzalez-Schlegel steepest descent path [25,26] in the mass weighted Cartesian coordinates with a step size of 0.01 $(\text{amu})^{1/2}$bohr. Force constants at 21 selected points (11 points in the reactant channel and 10 points in the products channel from $s = -1.5$ to 1.5 $\text{amu}^{1/2}$bohr) along the MEP were determined to obtain the necessary potential energy surface information for CVT calculations [27–29]. The points were chosen based on the curvatures of the MEP and the geometrical parameters as functions of the reaction coordinate according to our auto-focusing technique [30]. Energetic information along the MEP was further refined by the single point calculations using the coupled cluster method including single and double excitations with a quasi-perturbative triples contribution [CCSD(T)] [31] with the cc-pVDZ basis set at the BH&HLYP/cc-pVDZ geometries, which is denoted as [CCSD(T)/cc-pVTZ//BH&HLYP/cc-pVDZ]. The CCSD(T) energies, combined with the BH&HLYP/cc-pVDZ geometries and frequencies, were then used for the rate constant calculations.

TST/Eckart rate constants for all reactions in the above representative reaction set were calculated employing the kinetic module of the web-based Computational Science and Engineering Online (CSEO) program [32]. In these calculations, overall rotations were treated classically and vibrations were treated quantum mechanically within the harmonic approximation except for the modes corresponding to the internal rotations of the methyl (CH_3) and formyl radical (CHO) groups, which were treated as hindered rotations using the method suggested by Ayala et al. [33]. The thermal rate constants were calculated in the temperature range of 300–3,000 K, which is sufficient for many combustion applications such as premixed flame and shock-tube simulations. RC-TST parameters are derived from these rate constant calculations.

3 Results and discussion

3.1 CHO + CH_4 → HCHO + CH_3 reaction

Although the principal CHO + CH_4 reaction is not chosen as the reference reaction as discussed below, it is of great interest because it is the smallest reaction in the class and thus its rate constants can be obtained accurately from first-principles.

3.1.1 Stationary points

The optimized geometrical parameters of the reactants (CHO and CH_4) and products (HCHO and CH_3) at the BH&HLYP/cc-pVDZ and QCISD/cc-pVDZ levels of theory are shown in Fig. 1. The available experimental data are also given in parentheses. Geometrical parameters of the transition state are also given in Fig. 1 and Table 1. The transition state was confirmed by normal-mode analysis to have only one imaginary frequency whose mode corresponds to the transfer of the hydrogen atom from CH_4 to CHO. From Fig. 1 and Table 1, it is seen that the BH&HLYP/cc-pVDZ method gives optimized geometries close to those from the QCISD/cc-pVDZ level of theory for the reactants, products and transition state, especially for the reactive moiety with the largest difference of 0.02 Å. For the frequency calculations, the results from the BH&HLYP are also in excellent agreement with those calculated at the QCISD/cc-pVDZ; the averaged absolute difference between the two methods is about 30 cm^{-1}. It is noted that the performance of the B3LYP level of theory is worse than that of the BH&HLYP in both geometry optimization and frequency calculation for this reaction (see Table 1). The potential barriers and reaction energies from all the methods with ZPE corrections calculated at various levels of theory are listed in Table 2. It is expected that the compound method CBS-APNO [34] gives the most accurate result for barrier height and reaction energy, namely 25.29 and 17.00 kcal/mol, respectively. It is interesting to note that all the methods, except B3LYP, predict the barrier height from 25 to 27.5 kcal/mol and the reaction energy from 15.9 to 17.0 kcal/mol. B3LYP performs the worst as this method under-estimates the barrier height by 3.6 kcal/mol and over-estimates the reaction energy by 1.1 kcal/mol relative to the CBS-APNO values. This is, in fact, consistent with the previous finding that BH&HLYP performs well for transition state

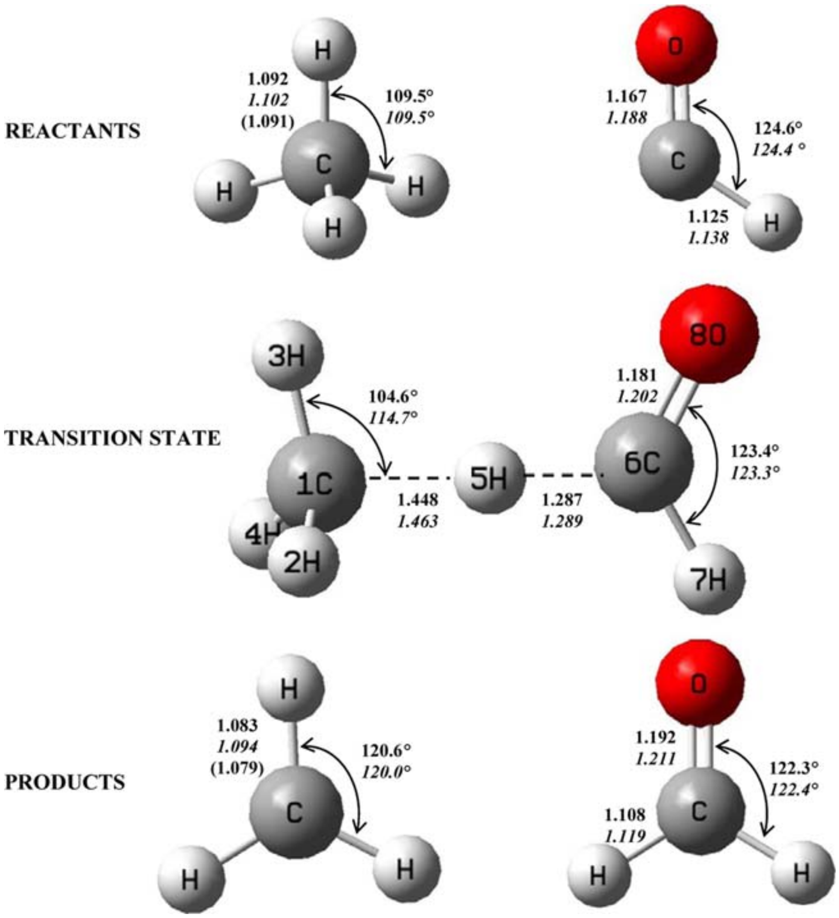

Fig. 1 Optimized geometries (distances in Å and angles in degrees) of the reactants, transition state and products at the BH&HLYP/cc-pVDZ and QCISD/cc-pVDZ (*italic numbers*). The numbers in the parentheses are the experimental values from reference [37]

properties in comparison to more accurate results [21–23]. It is noted that calculated $\Delta H^{\circ}_{\mathrm{rxn}}(298\,\mathrm{K})$ of 16.1 kcal/mol at the BH&HLYP/cc-pVDZ level is within the deviation of the available data of 14.6–16.9 kcal/mol [35]. To compromise the accuracy and computational efficiency, the CCSD(T)/cc-pVTZ//BH&HLYP/cc-pVDZ method is used to correct the energy along the minimum energy path for the CHO + CH_4 reaction for rate calculations below. It is noted that the difference in barrier height and reaction energy between the CBS-APNO and CCSD(T)/cc-pVTZ//BH&HLYP/cc-pVDZ methods is only about 0.7 kcal/mol.

3.1.2 Rate constants

The rate constants of the forward reactions were calculated using the canonical variational transition state theory (CVT) with the SCT, ZCT, and hindered rotor corrections in the temperature range of 300–3,000 K. Geometries and vibrational frequencies at the selected points along the MEP at the BH&HLYP level were used. The corresponding energy is from CCSD(T)/cc-pVTZ//BH&HLYP/cc-pVDZ. The internal rotation of the methyl group (or CHO group) was treated using the hindered rotor treatment suggested by Ayala et al. [33].

The calculated rate constants at different methods along with the tunneling and hindered rotation correction factors are listed in Table 3. Figure 2 shows the Arrhenius plot of calculated rate constants from the TST/Eckart/HR and CVT/SCT/HR (HR denotes hindered rotor), and available data in the literature. First, treatment of the motions of the methyl group (or formyl group) around the symmetry rotational axis as a hindered rotor rather than a harmonic oscillator proportionally decreases the rate constants as the temperature increases. In particular, it affects the rate constants by 66 and 85% at room temperature and at 3,000 K, respectively. Table 3 also lists the tunneling transmission coefficients calculated using one-dimensional Eckart, multi-dimensional zero-curvature ZCT, and small-curvature SCT methods. The overall tunneling contribution as predicted by the SCT method is significant, particularly at a lower temperature range. In particular, at 400 K, tunneling enhances the rate by a factor of 7.3 whereas it enhances the rate by a factor of 13.8 at 300 K. It is important to point out that the $CHO + CH_4 \rightarrow HCHO + CH_3$ reaction belongs to the H–L–H (heavy–light–heavy) reaction type. Also for such a reaction

Table 1 Optimized geometries and calculated harmonic frequencies of the transition state of the CHO + CH_4 reaction (distances are in Å and angles are in degree)

	B3LYP/cc-pVDZ	BH&HLYP/cc-pVDZ	QCISD/cc-pVDZ
1C-5H	1.53	1.45	1.46
5H-6C	1.26	1.29	1.29
∠1C-5H-6C	177.1	176.0	175.6
ω (cm^{-1})	1162i, 26, 138, 260, 491, 550, 563, 1,079, 1,246, 1,263, 1,388, 1,393, 1,456, 1,857, 2,777, 3,060, 3,217, 3,222	1814i, 27, 139, 282, 486, 590, 615, 1,126, 1,287, 1,328, 1,441, 1,453, 1,503, 1,948, 2,902, 3,146, 3,300, 3,306	1848i, 31, 127, 273, 484, 577, 610, 1,110, 1,263, 1,293, 1,425, 1,436, 1,491, 1,837, 2,853, 3,084, 3,235, 3,239

Table 2 Calculated barrier height and reaction energy for the CHO + CH_4 reaction (numbers are in kcal/mol)

Level of theory	ΔE	$\Delta V^{\neq}$
B3LYP/cc-pVDZ	18.10	21.69
BH&HLYP/cc-pVDZ	15.89	25.11
CCSD(T)/cc-pVTZ//BH&HLYP/cc-pVDZ	16.28	26.06
QCISD/cc-pVDZ	16.62	27.48
CBS-APNO	17.00	25.29

Zero-point energy correction is included

type it is known that due to the large curvature of the potential energy surface along the reaction coordinate, the small curvature tunneling approximation tends to underestimate the tunneling contributions particularly at low temperatures, e.g., $T < 300$ K due to the large corner cutting effects. However, since we are interested only in the temperature range that is important for combustion, i.e., 300–3,000 K, the SCT method should be sufficient. The comparison between our theoretical and suggested data is also shown in Fig. 2. The suggested data are obtained on the basis of the reverse process and the equilibrium constant in the absence of direct experimental measurement [6]. To the best of our knowledge, there is no theoretical study on rate constants for this reaction. Our calculated rate constants at various levels of theory agree well with the suggested data despite a large uncertainty factor of 5. Our most accurate CVT/SCT/HR rate constants were fitted to an Arrhenius expression and are given by:

$$k_p = 1.06 \times 10^{-24} \times T^{3.78} \times \exp\left(-\frac{10{,}744}{T}\right), \text{cm}^3\text{molecule}^{-1}\,\text{s}^{-1} \qquad (7)$$

3.2 CHO + C_2H_6 → HCHO + C_2H_5 reaction

In our previous studies [10,11], we pointed out that for reactions with hydrocarbons, reaction with ethane is the better reference reaction. To use the CHO + C_2H_6 reaction as the reference reaction, its thermal rate constants are needed. This is done by carrying out the conventional TST calculation for the CHO + C_2H_6 reaction with explicit treatment of both the methyl and formyl internal rotations as hindered rotors. The barrier used in the rate calculation is obtained from scaling that of reaction R_1 at CCSD(T)/cc-pVTZ//BH&HLYP/cc-pVDZ using the barrier heights of R_1 and R_2 at the BH&HLYP/cc-pVDZ level of theory which are given in Table 4. The barrier obtained is 24.88 kcal/mol. The tunneling contribution is obtained by scaling the κ^{SCT} of the CHO + CH_4 reaction by the scaling factor f_κ from Eq. 3. The resulting rate constants for the CHO + C_2H_6 reaction in the Arrhenius form are given by:

$$k_r = 3.74 \times 10^{-24} \times T^{3.74} \times \exp\left(-\frac{8,521}{T}\right), \text{cm}^3\text{molecule}^{-1}\,\text{s}^{-1} \qquad (8)$$

Figure 3 shows that our calculated rate constants are comparable to available suggested data [6] which are calculated on the basis of the estimated rate parameters for the reverse process and the equilibrium constant.

3.3 RC-TST parameters

In the discussion below, we first describe how the LERs, BHGs and the RC-TST factors were derived using the above training set. Subsequently, several error analyses were performed in order to provide some estimates on the accuracy of the RC-TST method applied to this reaction class. The first error analysis is the direct comparison between the calculated rate constants with those available in the literature for reactions R_3 & R_4. The second error analysis is the comparison between rate constants calculated by the RC-TST method and those from explicit full TST/Eckart calculations for the whole training set. The final analysis is on the systematic errors caused by introducing approximations in the RC-TST method.

Table 3 Hindered rotor (HR) correction factor, tunneling corrections factors $\kappa(T)$ and thermal rate constants $k(T)$ (cm^3 molecule^{-1} s^{-1}) for the CHO + CH_4 → HCHO + CH_3 reaction

$T(K)$	HR	$\kappa(T)$			$k(T)$			
		Eckart	ZCT	SCT	k^{TST}	k^{CVT}/k^{TST}	$k^{TST/SCT/HR}$	$k^{CVT/SCT/HR}$
300	0.44	43.38	6.76	13.81	2.78×10^{-31}	0.47	5.36×10^{-30}	7.97×10^{-31}
400	0.39	13.88	4.12	7.26	1.67×10^{-28}	0.44	9.02×10^{-28}	2.08×10^{-28}
500	0.35	7.07	2.97	4.71	2.14×10^{-26}	0.43	5.28×10^{-26}	1.50×10^{-26}
600	0.32	4.62	2.37	3.46	9.71×10^{-25}	0.42	1.44×10^{-24}	4.49×10^{-25}
700	0.30	3.48	2.02	2.76	2.14×10^{-23}	0.41	2.21×10^{-23}	7.13×10^{-24}
800	0.28	2.46	1.63	2.04	2.40×10^{-21}	0.39	1.64×10^{-21}	5.32×10^{-22}
900	0.26	1.76	1.31	1.50	1.09×10^{-18}	0.36	5.07×10^{-19}	1.57×10^{-19}
1,000	0.25	1.51	1.18	1.29	5.19×10^{-17}	0.34	1.96×10^{-17}	5.72×10^{-18}
1,500	0.21	1.28	1.07	1.11	1.32×10^{-14}	0.32	3.45×10^{-15}	9.51×10^{-16}
2,000	0.18	1.19	1.03	1.05	2.81×10^{-13}	0.30	5.91×10^{-14}	1.59×10^{-14}
2,500	0.16	1.14	1.01	1.02	2.08×10^{-12}	0.30	3.79×10^{-13}	1.00×10^{-13}
3,000	0.15	1.12	1.00	1.01	8.82×10^{-12}	0.29	1.43×10^{-12}	3.74×10^{-13}

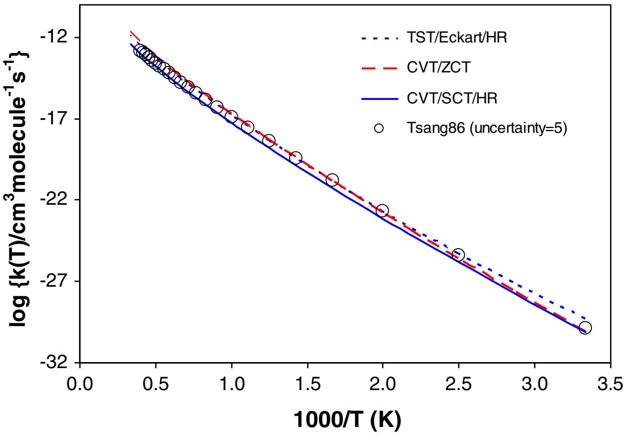

Fig. 2 Arrhenius plots of the calculated and available rate constants for the CHO + CH_4 → HCHO + CH_3

3.3.1 Calculation of potential energy factor

Note that for reactions with alkanes larger than ethane, such as propane C_3H_8, the three hydrogen atoms of the primary carbon atoms are not equivalent for abstraction by a CHO radical and thus the barrier heights of reactions at non-equivalent hydrogen atoms are different by about 0.7 kcal/mol at the BH&HLYP/cc-pVDZ level of theory. For simplicity within the RC-TST methodology, we assume that these hydrogen atoms are equivalent with the barrier height for abstractions taken to be the average value. Similar approximations are used for calculating other reaction class factors in this case. We found that such approximations only introduce a small error in our previous study [10]. The errors from such approximations are part of the systematic errors of the RC-TST method that will be discussed later.

The potential energy factor can be calculated using Eq. 6, where $\Delta V_a^{\neq}$ and $\Delta V_r^{\neq}$ are the barrier heights of the arbitrary and reference reactions, respectively. We have also shown that within a given class there is a linear energy relationship (LER) between the barrier heights and the reaction energies, similar to the well-known Evans-Polanyi linear free energy relationship [15–17]. Thus, with an LER, accurate barrier heights can be predicted from only the reaction energies. In this study the LER is determined where the reaction energies can be calculated by either the AM1 or the BH&HLYP level of theory. Moreover, for this reaction class, it is found that the barrier heights can also be grouped together depending on the abstraction sites, namely primary, secondary or tertiary, which was not observed previously in other reaction classes [8,10,11].

The reaction energies and barrier heights for all representative reactions in the training set are given explicitly in Table 4. The reaction barrier heights calculated at the BH&HLYP/cc-pVDZ level and the observed linear energy relationships plotted against the reaction energies calculated at the BH&HLYP/cc-pVDZ and AM1 levels are shown in Fig. 4a and b, respectively. The linear fit was obtained using the least square fitting method using the barrier heights and reaction energies calculated at the BH&HLYP/cc-pVDZ level of theory; it has the following expression in the energy units of kcal/mol:

$$\Delta V^{\neq} = 0.5611 \times \Delta E^{BH\&HLYP} + 16.49 \tag{9a}$$

The fitting expression using barrier heights at the BH&HLYP/cc-pVDZ level and reaction energies at the AM1 level of theory is also given as:

$$\Delta V^{\neq} = 0.3542 \times \Delta E^{AM1} + 22.50 \tag{9b}$$

Table 4 Reaction energies, barrier heights and absolute deviations between calculated barrier heights from the DFT and semi-empirical calculations and those from the LER expressions and the BHG approach

Reaction	ΔE		$\Delta V^{\neq}$				$\left\lvert\Delta V^{\neq} - \Delta V^{\neq}_{\text{estimated}}\right\rvert^{\text{f}}$		
	DFT [a]	AM1 [b]	DFT [a]	DFT [c]	AM1 [d]	BHG [e]	DFT [c]	AM1 [d]	BHG [e]
R_1	16.80	9.28	26.74						
R_2	12.86	3.44	24.03	23.71	23.72	23.83	0.32	***0.31***	0.20
R_3	13.23	3.59	23.79	23.91	23.77	23.83	0.13	0.02	0.04
R_4	9.58	−1.82	22.09	21.87	21.85	22.01	0.23	0.24	0.08
R_5	13.17	3.56	23.76	23.88	23.76	23.83	0.12	0.00	0.07
R_6	9.80	−1.59	21.71	21.99	21.93	22.01	0.28	0.23	***0.30***
R_7	13.39	4.13	23.77	24.00	23.96	23.83	0.23	0.19	0.06
R_8	6.90	−6.23	20.43	20.36	20.29	20.38	0.07	0.14	0.05
R_9	13.18	3.57	23.74	23.89	23.76	23.83	0.14	0.02	0.09
R_{10}	9.74	−1.61	21.96	21.96	21.93	22.01	0.00	0.04	0.05
R_{11}	9.99	−1.23	21.93	22.10	22.06	22.01	0.17	0.13	0.08
R_{12}	13.22	4.15	23.83	23.91	23.97	23.83	0.08	0.14	0.00
R_{13}	7.27	−6.02	20.32	20.57	20.37	20.38	0.25	0.04	0.05
R_{14}	9.60	−1.19	22.04	21.88	22.08	22.01	0.16	0.04	0.02
R_{15}	12.45	3.36	23.91	23.48	23.69	23.83	***0.43***	0.22	0.07
MAD[g]							**0.19**	**0.13**	**0.09**

Zero-point energy correction is not included

Energies are kcal/mol

[a] Calculated at the BH&HLYP/cc-pVDZ level of theory

[b] Calculated at the AM1 level of theory

[c] Calculated from the LER using reaction energies calculated at the BH&HLYP/cc-pVDZ level of theory: Eq. 9a

[d] Calculated from the LER using reaction energies calculated at the AM1 level of theory: Eq. 9b

[e] Estimated from the BHG

[f] $\Delta V^{\neq}$ from the BH&HLYP/cc-pVDZ calculations; $\Delta V^{\neq}_{\text{estimated}}$ from the LER using the BH&HLYP/cc-pVDZ and AM1 reaction energies or from the BHG

[g] Mean absolute deviations (MAD) for reaction R_2–R_{15}

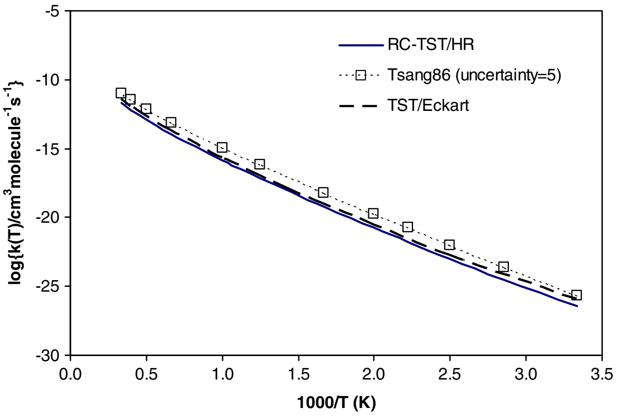

Fig. 3 Arrhenius plots of the calculated and available rate constants for the $CHO + C_2H_6 \rightarrow HCHO + C_2H_5$

The absolute deviations of reaction barrier heights between the LERs and the direct DFT BH&HLYP/cc-pVDZ calculations are smaller than 0.45 kcal/mol (see Table 4). The mean absolute deviation of reaction barrier heights predicted from the BH&HLYP and AM1 reaction energies are 0.19 and 0.13 kcal/mol, respectively. These deviations are in fact smaller than the systematic errors of the computed reaction barriers from full electronic structure calculations. Note that in the RC-TST/LER methodology only the relative barrier height is needed. To compute these relative values, the barrier height of the reference reaction R_2 calculated at the same level of theory, i.e., BH&HLYP/cc-pVDZ, is needed and has the value of 24.03 kcal/mol (see Table 4).

Based on the observation of barrier heights grouping (BHG) on the type of carbon site, the average values are assigned to all reactions in the same type of site, particularly 23.83, 22.01 and 20.38 kcal/mol for primary, secondary and tertiary carbon sites, respectively. The maximum and the averaged deviations of reaction barrier heights estimated from grouping are 0.30 and 0.09 kcal/mol, respectively. In fact they are smaller than those obtained from the LERs. Therefore it is recommended that the barrier heights should

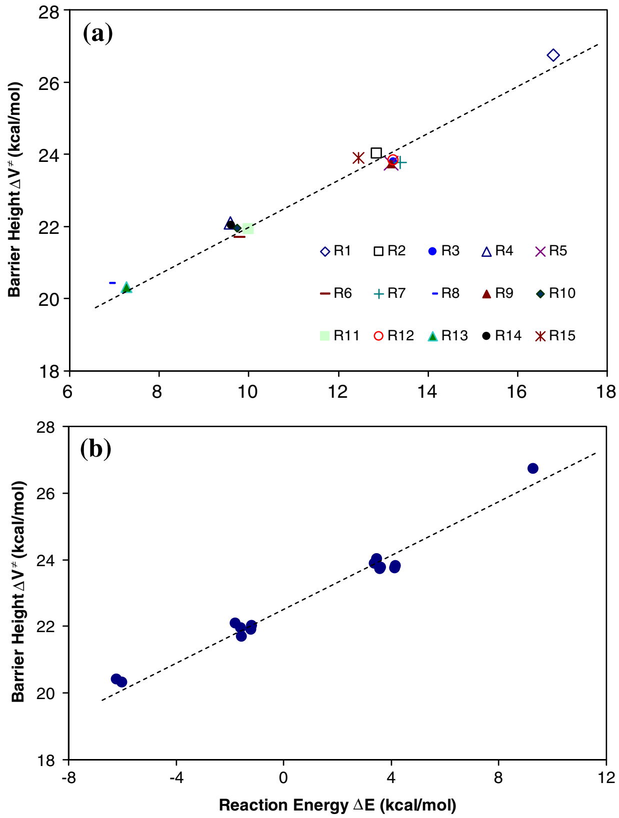

Fig. 4 Linear energy relationship plots of the barrier heights, $\Delta V^{\neq}$, versus the reaction energies ΔE. Barrier heights were calculated at the BH&HLYP/cc-pVDZ level of theory. ΔE's were calculated at **a** the BH&HLYP/cc-pVDZ and **b** the AM1 level of theory

be estimated using the latter approach. It is worth noting that in the BHG approach no additional information is needed in order to estimate rate constants.

In conclusion, the barrier heights for any reaction in this reaction class can be obtained by using either the LER or BHG approach. The estimated barrier height is then used to calculate the potential energy factor using Eq. 6. The performance for such estimations on the whole representative reaction set is discussed in the error analyses below.

3.3.2 Calculation of symmetry number factor

The symmetry number factors f_σ were calculated simply from the ratio of reaction symmetry numbers of the arbitrary and reference reactions using Eq. 3 and are listed in Table 5. The reaction symmetry number of a reaction is given by the number of symmetrically equivalent reaction paths. It can be easily calculated from the rotational symmetry numbers of the reactant and the transition state [30], thus this factor can be calculated exactly.

3.3.3 Calculation of tunneling factor

The tunneling factor f_κ is the ratio of the transmission coefficient of reaction R_a to that of reaction R_r. Due to cancellation of errors in calculations of the tunneling factors, we have shown that the factor f_κ can be reasonably estimated using the one-dimension Eckart method [36]. Calculated results for the representative set of reactions can then be fitted to an analytical expression. It was observed in this study, as well as in our previous work [8], that tunneling factors for hydrogen abstraction reactions at the same sites - primary, secondary or tertiary carbon sites - are rather similar and thus can be assumed to be the same for each kind of carbon site. Simple expressions for the three tunneling factors for abstraction at the primary, secondary and tertiary carbon sites, respectively, are obtained by fitting to the calculated values and are given below:

$$f_\kappa = 1 - 5.13 \times \exp\left(-0.0128 \times T\right) \quad \text{for primary carbon sites} \tag{10a}$$

$$f_\kappa = 1.006 \times \exp\left[5.74 \times 10^{6} \times T^{-2.89}\right] \quad \text{for secondary carbon sites} \tag{10b}$$

$$f_\kappa = 1.010 \times \exp\left[5.05 \times 10^{7} \times T^{-3.22}\right] \quad \text{for tertiary carbon sites} \tag{10c}$$

The correlation coefficients for these fits are larger than 0.999. The three equations are plotted in Fig. 5. Table 5 also lists the error analysis of tunneling factors at 300 K. It can be seen that the same tunneling factor expression can be reasonably assigned to those reactions at the same site with the largest absolute deviation of 0.14 and the largest percentage deviation of 13.41% for R_{15}; also the mean absolute deviation is 4.18%, compared to the direct Eckart calculation using reaction information from the BH&HLYP/cc-pVDZ level of theory. At higher temperatures, tunneling contributions to the rate constants decrease and thus, as expected, the differences between the approximated values and the explicitly calculated ones also decrease; for example, the maximum error for all reactions is less than 3 % at 500 K.

3.3.4 Calculation of partition function factor

The partition factor includes translational, rotational, internal rotation, vibrational, and electronic component. As pointed out in our previous study [8], the partition function factor f_Q mainly originates from the differences in the coupling between the substituents with the reactive moiety and its temperature dependence arises from the vibrational component and internal rotations only. For this reaction class, there are two kinds of internal rotors, namely rotation of the CHO group along the C–C bond at the transition state and rotation

Table 5 Calculated symmetry number factors and tunneling factors at 300 K

Reaction	Symmetry number factor	Tunneling ratio factor, f_κ			
		Eckart [a]	Fitting [b]	Deviation [c]	Deviation [d](%)
R_2	1.000	(90.62) [f]	–	–	–
R_3	1.000	0.88	0.90	0.03	2.97
R_4	0.333	1.56	1.47	0.08	5.27
R_5	1.000	0.89	0.90	0.02	1.81
R_6	0.667	1.47	1.47	0.01	0.50
R_7	1.500	0.84	0.90	0.06	7.07
R_8	0.167	1.78	1.69	0.09	5.19
R_9	1.000	0.83	0.90	0.07	8.56
R_{10}	0.667	1.47	1.47	0.01	0.46
R_{11}	0.333	1.45	1.47	0.02	1.57
R_{12}	1.000	0.88	0.90	0.02	2.17
R_{13}	0.167	1.66	1.69	0.03	1.57
R_{14}	0.333	1.53	1.47	0.06	3.72
R_{15}	0.500	1.04	0.90	0.14	13.41
MAD[e]				**0.05**	**4.18**

[a] Calculated directly using the Eckart method with the BH&HLYP/cc-pVDZ reaction barrier heights and energies

[b] Calculated by using fitting expression (see Eqs. 10a–10c)

[c] Absolute deviation between the fitting and directly calculated values

[d] Percentage deviation (%)

[e] Mean absolute deviations (MAD) and deviation percentage between the fitting and directly calculated values

[f] Tunneling coefficient calculated for reaction (R_2) using the Eckart method with the energetic and frequency information at the BH&HLYP/cc-pVDZ

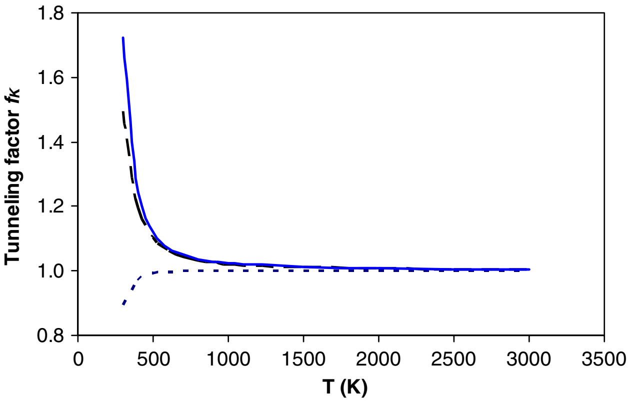

Fig. 5 Plots of the tunneling factor f_κ as a function of temperature for abstractions of hydrogen from primary (*dotted line*), secondary (*dashed line*), and tertiary (*solid line*) carbon sites

of the alkyl group such as CH_3 along the C–C bond at both the transition states and the reactant alkanes, that need to be treated as hindered rotations. We used the approach proposed by Ayala et al. [33] for treating hindered rotations. Note that the reference reaction R_2 has both the CHO and CH_3 internal rotations. Thus, the reaction class factor due to these hindered rotations is a measure of the substituent effects on the rate constant from these hindered rotors relative to that of the reference R_2 reaction. For simplicity, the hindered corrections are added into the harmonic partition function. It is found that the total partition function for these reactions in the training set separates into two groups: reactions at (1) the primary carbon site and (2) secondary and tertiary sites. For simplicity, the average values for the two groups are considered and fitted into linear expressions as given below:

$$f_Q = 0.087 + 0.00020 \times T \text{ for the primary carbon sites} \quad (11a)$$

$$f_Q = 0.323 + 0.00016 \times T \text{ for the secondary and tertiary carbon sites} \quad (11b)$$

They are plotted for 13 reactions (for reaction R_3–R_{15}) in the class in the temperature range 300–3,000 K, given in Fig. 6. The deviation for all training reactions in the groups are averaged at each temperature and then plotted in Fig. 7.

3.3.5 Prediction of rate constants

What we have established so far are the necessary parameters - namely potential energy factor, symmetry number factor, tunneling factor and partition function factor - for application of the RC-TST theory to predict rate constants for any reaction in the CHO + Alkane class. The procedure for calculating the rate constants of an arbitrary reaction in this class is: (1) calculate the potential energy factor using Eq. 6 with the $\Delta V_r^{\neq}$ value of 24.03 kcal/mol. The reaction barrier height can be obtained using the BHG approach or using the LER approach by employing Eq. 9a for BH&HLYP/cc-pVDZ or Eq. 9b for AM1 reaction energies; (2) calculate the symmetry number factor from Eq. 3 or see Table 5; (3) compute the tunneling factor using Eq. 10a, 10b and 10c for

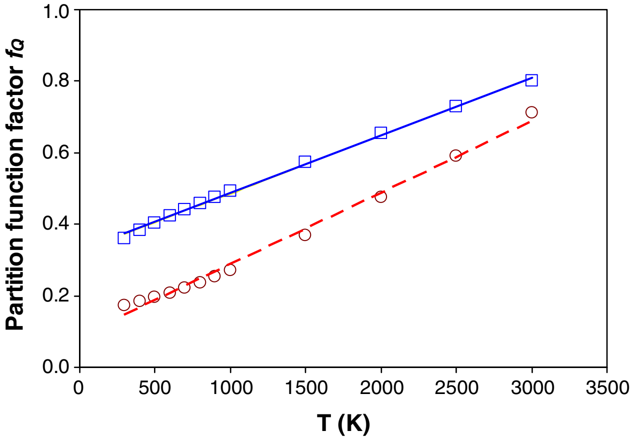

Fig. 6 Plots of the partition function factor f_Q as a function of the temperature for 13 considered reactions, R_3–R_{15}. The *solid line* is the fitting line for average value of partition function at secondary and tertiary sites (*open squares*) and *dashed line* is for primary carbon site (*open circles*). Hindered rotation treatment is included

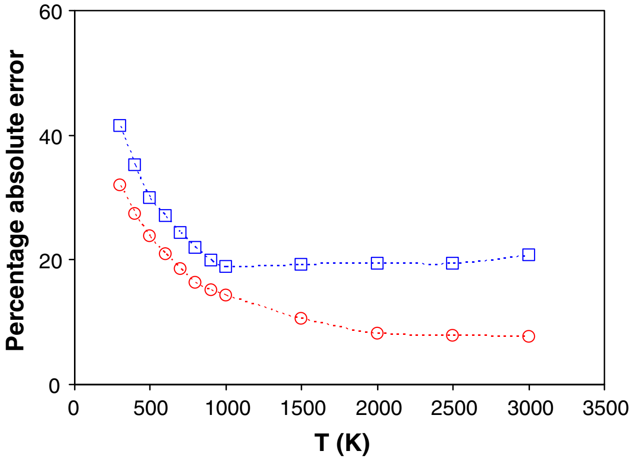

Fig. 7 The same as Fig. 6 but for the absolute error in estimating partition function factor

primary, secondary and tertiary carbon sites, respectively; (4) evaluate the partition function factor using Eq. 11a or 11b; and (5) the rate constants of the arbitrary reaction can be calculated by taking the product of the reference reaction rate constant given by Eq. 8 with the reaction class factors above. Table 6 summarizes the RC-TST parameters for this reaction class.

For comparison with available rate constants in the literature we selected two reactions R_3 and R_4 whose rate constants have been suggested from a literature review. It is noted that there is no previous theoretical calculation or direct experimental data available for these reactions. Figure 8a–b show the predicted rate constants of reaction R_3 and reaction R_4 using the RS-TST method and suggested data [5]. It is seen that the rate constants calculated using the RC-TST/LER are not much different from RC-TST/BHG for these two reactions. The RC-TST predicts values lower than the suggested data. It is noted that this comparison only gives a quantitative picture about the performance of this approach because of the uncertainty of the available literature rate constants for these two reactions.

A better analysis on the efficiency of the RC-TST method would be to compare the RC-TST results with explicit theoretical calculations. As mentioned in our previous studies [8,9,14], the RC-TST methodology can be thought of as a procedure for extrapolating rate constants of the reference reaction to those of any given reaction in the class. Comparisons between the calculated rate constants for a small number of reactions using both the RC-TST and the full TST/Eckart methods would provide additional information on the accuracy of the RC-TST method. To be consistent, the TST/Eckart rate constants of the reference reaction were used in calculation of RC-TST rate constants for this particular analysis rather than using the expression in Eq. 8. The results for this error analysis for 13 representative reactions (i.e., the comparisons between the RC-TST/BHG and full TST/Eckart methods) are shown in Fig. 9. Here we plotted the relative deviation defined by ($|k^{\mathrm{TST/Eckart}}$-$k^{\mathrm{RC\text{-}TST/HBG}}|/k^{\mathrm{TST/Eckart}}$) as a percentage versus the temperature for several selected reactions. The relative errors are less than 60 % for all test cases; thus it can be concluded that the RC-TST can predict thermal rate constants for reactions in this class within a factor of two when compared to those calculated explicitly using the TST/Eckart method. The comparison using the RC-TST/LER is similar to that of RC-TST/BHG with no significant difference.

Finally, we examined the systematic errors in different factors in the RC-TST/LER and the RC-TST/BHG methods. The total error is affected by the errors in the approximations in the potential energy factor, tunneling factor and partition function factor introduced in the method. It is noted that the symmetry number factor is "exact", but the error for the partition function factor does include the error in the approximation for the hindered rotation treatment. The deviations/errors between the approximated and exact factors are calculated at each temperature for every reaction in the training set and then averaged over the whole class. The error in the potential energy factor comes from the use of an LER expression as in Eqs. 9a and 9b or from taking the average value for reactions at each site; that of the tunneling factor, from using three Eqs. 10a–10c; and that of the partition function factor, from using Eqs. 11a or 11b. The results of the analysis on the errors from different relative rate factors, namely f_κ, f_Q, and f_V, used in the RC-TST method are shown in Fig. 10. The errors in f_V from using the LER are higher than the grouping approximation but the difference is not significant, especially at high temperatures. In this figure, we plotted the absolute errors averaged over all 13 reactions as functions of temperature. Of the three factors, errors from the

Table 6 Parameters and Formulations of the RC-TST Method for the CHO + Alkane → HCHO + Alkyl Reaction Class (CHO + C_2H_6 is the reference reaction)

$k(T) = f_\sigma \times f_\kappa(T) \times f_Q(T) \times f_v(T) \times k_r(T)$; $f_v(T) = \exp\left[\frac{-(\Delta V^{\neq} - \Delta V_r^{\neq})}{k_B T}\right]$		
f_σ	Calculated explicitly from the symmetry of reactions (see Table 5)	
$f_\kappa(T)$	$1 - 5.13 \times \exp(-0.0128 \times T)$ for primary carbon	
	$1.006 \times \exp\left[5.74 \times 10^6 \times T^{-2.89}\right]$ for secondary carbon	
	$1.010 \times \exp\left[5.05 \times 10^7 \times T^{-3.22}\right]$ for tertiary carbon	
$f_Q(T)$	$0.087 + 0.00020 \times T$ for primary carbon	
	$0.323 + 0.00016 \times T$ for secondary and tertiary carbon	
$\Delta V^{\neq}$	BHG	23.83 kcal/mol for primary carbon
		22.01 kcal/mol for secondary carbon
		20.38 kcal/mol for tertiary carbon
	LER	$0.5611 \times \Delta E^{\text{BH\&HLYP}} + 16.49$
		$0.3542 \times \Delta E^{\text{AM1}} + 22.50$
	$\Delta V_r^{\neq} = 24.03$ kcal/mol [a]	
$k_r(T)$	$k_r = 3.74 \times 10^{-24} \times T^{3.74} \times \exp\left(-\frac{8521}{T}\right)$, cm^3 molecule^{-1} s^{-1} (Eq. 8)	

T is in Kevin; $\Delta V^{\neq}$ and ΔE are in kcal/mol; Zero-point energy correction is not included

[a] Calculated value for the reaction R_2 at the BH&HLYP/cc-pVDZ level of theory

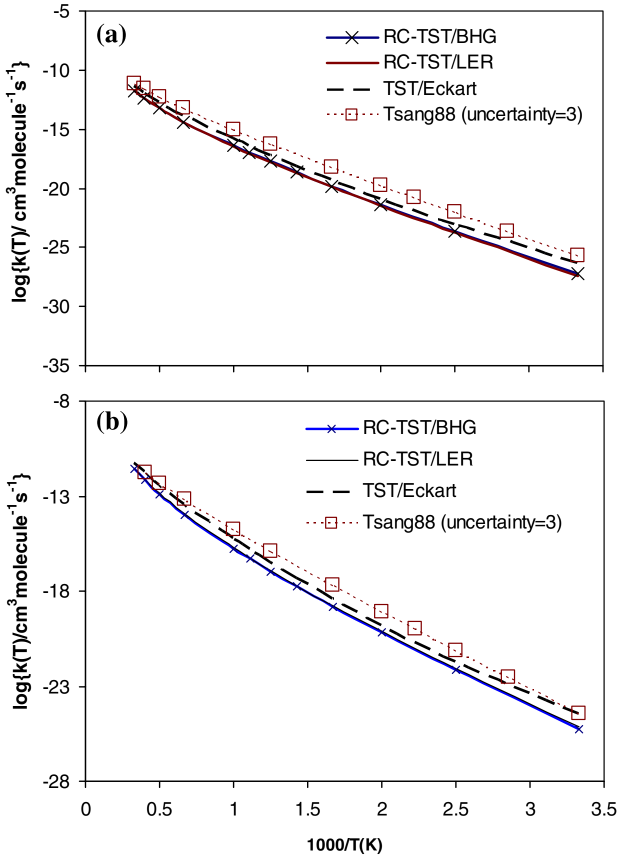

Fig. 8 Arrhenius plots of the calculated rate constants using the RC-TST methods for some representative reactions along with the available literature values as well as the calculated TST/Eckart rate constants: **a** CHO + C_3H_8 at primary carbon, and **b** CHO + C_3H_8 at secondary carbon

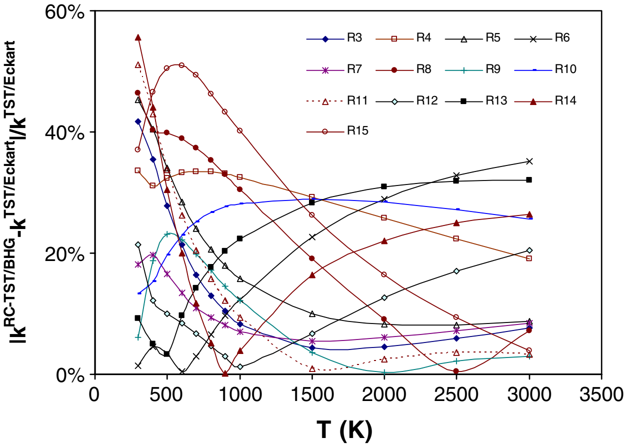

Fig. 9 Relative absolute deviations as functions of the temperature between rate constants calculated from the RC-TST/BHG and full TST/Eckart methods for all selected reactions

partition function factor are the largest, followed by those of the potential energy factor. Errors from all components are less than 40%. All errors tend to decrease when the temperature increases, and so does the error in the total factor. The total systematic errors due to the use of simple analytical expressions for different reaction class factors are less than 40% in the temperature range of 300–3,000 K.

4 Conclusion

We have extended our application of RC-TST combined with the LER or the BHG to the prediction of thermal rate constants for hydrogen abstraction reactions of the CHO + alkane class. The rate constants for the reference reaction, CHO + C_2H_6, are obtained explicitly using the RC-TST from those of the principal reaction, CHO+CH_4, which were previously

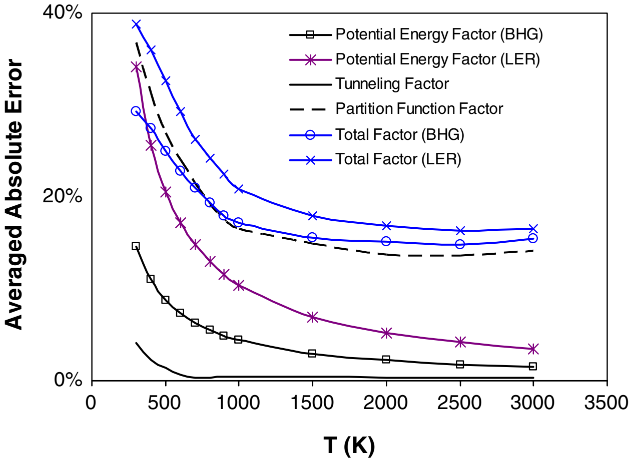

Fig. 10 Averaged absolute errors of the total relative rate factors f(T) (Eq. 2) and its components, namely the tunneling (f_K), partition function (f_Q), and potential energy (f_V) factors as a function of temperature

obtained by CVT calculation with ZCT, SCT and the hindered rotor model in the temperature range of 300–3,000 K. Combined with these data, both the RC-TST/LER, where only reaction energy is needed, and RC-TST/BHG, where no other information is needed, are found to be promising methods for predicting rate constants for a large number of reactions in a given reaction class. Our analysis indicates that the RC-TST/LER or the RC-TST/BHG method yield less than 40% systematic errors on the average in the predicted rate constants and less than 100% or a factor of 2 on the average when compared to explicit rate calculations. Consequently, this method should be useful for estimates of rate constants for reactions involved in complex combustion systems such as the combustion of hydrocarbons.

Acknowledgments This work is supported in part by the National Science Foundation. LKH is grateful to the Vietnam Education Foundation for a Graduate Fellowship. The authors would like to thank the Utah Center for High Performance Computing (CHPC) for computer time and support.

References

1. Curran HJ, Gaffuri P, Pitz WJ, Westbrook CK (2002) Combust Flame 129:253
2. Zhang H-Y, McKinnon JT (1995) Combust Sci Tech 107:261
3. Richter H, Howard JB (2002) Phys Chem Chem Phys 4:2038
4. Richter H, Granata S, Green WH, Howard JB (2005) Proc Combust Inst 30:1397
5. Tsang W (1988) J Phys Chem Ref Data 17:887
6. Tsang W, Hampson RF (1986) J Phys Chem Ref Data 15:1087
7. Tsang W (1990) J Phys Chem Ref Data 19:1
8. Zhang S, Truong TN (2003) J Phys Chem A 107:1138
9. Truong TN (2000) J Chem Phys 113:4957
10. Huynh LK, Ratkiewicz A, Truong TN (2006) J Phys Chem A 110:473
11. Kungwan N, Truong TN (2005) J Phys Chem A 109:7742
12. Truong TN, Duncan WT, Tirtowidjojo M (1999) Phys Chem Chem Phys 1:1061
13. Truong TN, Truong TTT (1999) Chem Phys Lett 314:529
14. Truong TN, Maity DK, Truong T-TT (2000) J Chem Phys 112:24
15. Polanyi JC (1972) Acc Chem Res 5:161
16. Evans MG, Polanyi M (1936) Trans Faraday Soc 32:1333
17. Evans MG, Polanyi M (1936) Proc R Soc 154:133
18. Frisch MJ, Trucks GW, Schlegel HB, Scuseria GE, Robb MA, Cheeseman JR, Montgomery JA, Jr. TV, Kudin KN, Burant JC, Millam JM, Iyengar SS, Tomasi J, Barone V, Mennucci B, Cossi M, Scalmani G, Rega N, Petersson GA, Nakatsuji H, Hada M, Ehara M, Toyota K, Fukuda R, Hasegawa J, Ishida M, Nakajima T, Honda Y, Kitao O, Nakai H, Klene M, Li X, Knox JE, Hratchian HP, Cross JB, Adamo C, Jaramillo J, Gomperts R, Stratmann RE, Yazyev O, Austin AJ, Cammi R, Pomelli C, Ochterski JW, Ayala PY, Morokuma K, Voth GA, Salvador P, Dannenberg JJ, Zakrzewski VG, Dapprich S, Daniels AD, Strain MC, Farkas O, Malick DK, Rabuck AD, Raghavachari K, Foresman JB, Ortiz JV, Cui Q, Baboul AG, Clifford S, Cioslowski J, Stefanov BB, Liu G, Liashenko A, Piskorz P, Komaromi I, Martin RL, Fox DJ, Keith T, Al-Laham MA, Peng CY, Nanayakkara A, Challacombe M, Gill PMW, Johnson B, Chen W, Wong MW, Gonzalez C, Pople JA (2003) Gaussian 03, Revision A.1, Gaussian, Inc., Pittsburgh
19. Becke AD (1993) J Chem Phys 98:1372
20. Lee C, Yang W, Parr RG (1988) Phys Rev 37:785
21. Truong TN (1994) J Chem Phys 100:14
22. Truong TN, Duncan W (1994) J Chem Phys 101:7408
23. Lynch BJ, Fast PL, Harris M, Truhlar DG (2000) J Phys Chem A 104:4811
24. Dunning TH Jr (1989) J Chem Phys 94:5523
25. Gonzalez C, Schlegel HB (1989) J Chem Phys 90:2154
26. Gonzalez C, Schlegel HB (1990) J Phys Chem 94:5523
27. Truhlar DG, Garrett BC (1980) Accs Chem Res 13:440
28. Truhlar DG, Isaacson AD, Garrett BC (1985) Generalized Transition State Theory. In: Baer M (ed) Theory of chemical reaction dynamics, vol 4. CRC Press, Boca Raton, p 65
29. Truhlar DG (1995) Direct dynamics method for the calculation of reaction rates. In: Heidrich D (ed) The reaction path in chemistry: current approaches and perspectives. Kluwer Academic, Dordrecht, p 229
30. Duncan WT, Bell RL, Truong TN (1998) J Comp Chem 19: 1039
31. Pople JA, Head-Gordon M, Raghavachari K (1987) J Chem Phys 87:5968
32. Truong TN http://www.cseo.net
33. Ayala PY, Schlegel HB (1998) J Chem Phys 108:2314
34. Ochterski JW, Petersson GA, Montgomery JA Jr (1996) J Chem Phys 104:2598
35. NIST Standard Reference Database Number 69, June 2005 Release, http://webbook.nist.gov/chemistry/
36. Miller WH (1979) J Am Chem Soc 101:6810
37. DeMore WB, Sander SP, Golden DM, Hampson RF, Kurylo MJ, Howard CJ, Ravishankara AR, Kolb CE, Molina MJ (1992) in JPL publication (Jet Propulsion Laboratory, Pasadena), pp 90